Iterative Lead Compensation Control of Nonlinear Marine Vessels Manoeuvring Models

Elías Revestido Herrero, M. Tomás-Rodríguez, and Francisco J. Velasco González, *Member, IEEE*

Abstract

This paper addresses the problem of control design and implementation for a nonlinear marine vessel manoeuvring model. The authors consider a highly nonlinear vessel 4 DOF model as the basis of this work. The control algorithm here proposed consists of a combination of two methodologies: $i)$ an iteration technique that approximates the original nonlinear model by a sequence of linear time varying equations whose solution converge to the solution of the original nonlinear problem and, $ii)$ a lead compensation design in which for each of the iterated linear time varying system generated, the controller is optimized at each time on the interval for better tracking performance. The control designed for the last iteration is then applied to the original nonlinear problem.

Simulations and results here presented show a good performance of the approximation methodology and also an accurate tracking for certain manoeuvring cases under the control of the designed lead controller. The main characteristic of the nonlinear system′s response are the reduction of the settling time and the elimination of the steady state error and overshoot.

Index Terms

control engineering, nonlinear systems, autopilot, lead compensation, course-keeping.

Elías Revestido Herrero is with the Dept. of Electronic Technology, Systems Engineering and Automatic Control, Universidad de Cantabria, Spain, (e-mail: revestidoe@unican.es).

M. Tomás-Rodríguez is with School of Engineering and Mathematical Sciences, City University London, United Kingdom, (e-mail: Maria.Tomas-Rodriguez.1@city.ac.uk).

Francisco J. Velasco González is with the Dept. of Electronic Technology, Systems Engineering and Automatic Control, Universidad de Cantabria, Spain, (e-mail: velascof@unican.es)

I. INTRODUCTION

The design of autopilots based on proportional-integral-derivative (PID) methodologies has been in use since $1920'$s [1] with the help of gyrocompasses which measured the vehicle$'$s heading angle for feedback purposes. The major challenges confronted in the design of ship autopilots are mainly the existing surrounding environmental uncertainties such as waves, wind, ocean currents and the high nonlinear ship dynamics. In addition to these, the rudder dynamics also present saturation-type nonlinearities on its rate and deflection angle.

Several articles deal with the design and implementation of PID based autopilots, in which linearizations for the vessel$'$s manoeuvring model are performed, see [1]–[6] as the most representative. In the case of low speed applications, it is acceptable to neglect the nonlinear dynamics on the ships manoeuvring model due to linear terms predomination. However, for high speed applications, tight turns, large sideslip angles or in the presence of currents, nonlinear effects become pronounced and thus neglecting them may degrade the controller$'$s performance and robustness.

On the other hand, different nonlinear methods [1] have been presented for course-keeping autopilots design such as state feedback linearization [7], nonlinear backstepping [8], [9], sliding mode control [10], output feedback [11], H_∞-control [12], particle swarm optimization [13], genetic algorithms [10], fuzzy logic methods [14],... etc. For most of these type of applications, nonlinear manoeuvring models in 1 degree of freedom (DOF) are considered, see [15] or [16] as example, still in these contributions, the coupling existing between the various variables is obviously not taken into account. Due to the complexity of some of the above cited nonlinear methods, the implementation may be tedious and time consuming from the computational point of view.

The aim of this article is to design a control method for a nonlinear marine vessel manoeuvring model without performing any simplification in the model$'$s nonlinearities or variable$'$s couplings. The authors propose a control strategy based on an optimized lead compensation control methodology combined with an iteration technique used to approach the original nonlinear system. This iteration technique was initially presented in [17], [18] and has been used to solve various nonlinear control problems such as optimal control [19], observers design [20], nonlinear optimal tracking [21],...etc. One of its advantages is the fact that it maintains the

inherent nonlinear characteristics of the system′s behaviour, providing the grounds for a robust control implementation where modelling uncertainties are removed. The iteration technique is applied to a 4 DOF nonlinear manoeuvring ship model. This opens the novel possibility of course-keeping autopilot design based on lead compensation methodology applied to a nonlinear model. This approach exist without the limitations of the linear models previously indicated, and keeps the simplicity of the lead compensation design and implementation. Furthermore, based on a preliminar study, the use of a lead controller instead of a conventional PID is justified. By an appropriate optimization technique, a trade off between the overshoot and time response is achieved without stationary state error.

The objective is to design a lead compensation controller for nonlinear systems of the form:

$$\dot{x} = f(x) = A(x)x(t) + B(x)u_c(t, \theta_c), \quad x(0) = x_0 \tag{1}$$

where $u_c(t, \theta_c)$ is the control action, θ_c is the set of controller′s parameters, $x(t)$ is the state vector, $A(x)$, $B(x)$ are matrices of appropriate dimensions and $x(0)$ are the initial conditions. Replacing the nonlinear system by a sequence of "i" linear time varying (LTV) systems, a sequence of corresponding feedback laws $u_c^{(i)}(t, \theta_c)$ is generated: for each of them, the closed-loop response for the i^{th} LTV system at each time of the time interval is controlled by the designed lead controller $u_c^{(i)}(t, \theta_c)$. From the convergence of the sequence of LTV solutions [17], the last iterated control law $u_c^{(i)}(t, \theta_c)$, (corresponding to the i^{th} iteration), will provide lead controller stability objectives satisfaction when it is applied to the nonlinear system.

The structure of the article is as follows: Section II contains the detailed description of the nonlinear model for the vessel under consideration. Details on the hydrodynamic, propulsion and control forces are given. Section III provides details on the iteration technique and the convergence theorem is stated. Section IV shows the application of this technique to the nonlinear vessel model by using a 20°-20° zig-zag manoeuvre example to illustrate the ideas. Section V presents the control algorithm design and implementation. Section VI shows the performance of the control methodology on the vessel′s nonlinear model. This section contains the simulations carried out and a discussion on the results obtained. Conclusions and further research guidelines are provided in section VII.

II. The Mathematical Model

The nonlinear dynamical model described in this section is classified as what is known as manoeuvring. Manoeuvring deals with the ship′s motion in absence of waves excitation (calm water) [22]. The motion results from the action of control devices such as control surfaces (rudders, fins, T-foils) and propulsion units.

In manoeuvring theory, the motion of 4 DOF ship models requires from four independent coordinates in order to fully determine the position and orientation of the vehicle, which is considered to be a rigid body. These coordinates represent the longitudinal and lateral positions and speeds as well as and their derivatives along the respective coordinate frames. The variables describing the vessels′s dynamics are provided in table I and figure 1 following the notation found in [23], which will be adopted for remaining of this article.
The four degrees of freedom under consideration in this work describe the ship′s motion (surge, sway and yaw) on the horizontal plane and the roll in the vertical plane. Two coordinate frames are used: the n coordinate system (earth-fixed), O_n, is used to define the ship position and the system b, (body-fixed) O_b, helps to define the ship′s orientation [22] (see figure 1).

TABLE I
NOTATION FOR THE SHIP′S DISPLACEMENT VARIABLES.

Movement	**Force**	**Linear Speed**	**Position**
Surge	X	u "b-frame"	x_n "n-frame"
Sway	Y	v "b-frame"	y_n "n-frame"
Rotation	**Moment**	**Angular Speed**	**Angle**
Roll	K	p "b-frame"	ϕ euler
Yaw	N	r "b-frame"	ψ(heading) euler

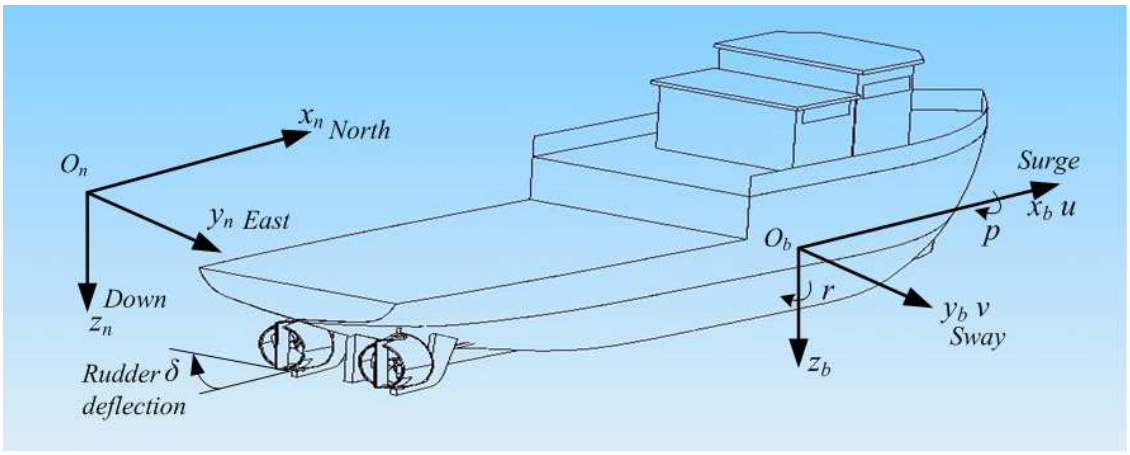

Fig. 1. Ship′s displacement variables and coordinate systems.

The rigid-body equations of motion of the 4 DOF model are given by [24]:

$$\begin{aligned} m[\dot{u} - y_g^b \dot{r} - vr - x_g^b r^2 + z_g^b pr] &= \tau_X \\ m[\dot{v} - z_g^b \dot{p} + x_g^b \dot{r} + ur - y_g^b (r^2 + p^2)] &= \tau_Y \\ I_{xx}\dot{p} - mz_g^b \dot{v} + m[y_g^b vp - z_g^b ur] &= \tau_K \\ I_{zz}\dot{r} + mx_g^b \dot{v} - my_g^b \dot{u} + m[x_g^b ur - y_g^b vr] &= \tau_N \end{aligned} \tag{2}$$

The subindex $_g$ refers to the center of gravity and the superindex ^{b} to the b-frame. Details of the parameters included in equations (2) can be found in Appendix A. These equations of motion are formulated about the b-frame, which is fixed to the point determined by the intersection of the port-starboard plane of symmetry, the waterline plane and the transverse vertical plane at $L_{pp}/2$ (see Appendix A for hull dimensions).

The force terms on the right hand side of equations (2) can be described as the total contribution of the hydrodynamic, propulsion and control forces:

$$\tau = \tau_{hyd} + \tau_p + \tau_c \tag{3}$$

These terms will be described next.

A. Hydrodynamic Forces

The hydrodynamic forces considered in this section, τ_{hyd}, are those appearing due to the motion of the vessel in calm water. The following equations correspond to the model established by [25] that proposed a simplified version of the model in [26], preserving in this way the most important hydrodynamic coefficients so that the model describes a wide variety of manoeuvring regimes in spite of some minor simplifications. Hydrodynamic forces are mainly composed by surge, sway, roll and yaw terms:

- *Surge terms*

$$\tau^b_{Xhyd} = X_{\dot{u}}\dot{u} + X_{vr}vr + X_{u|u|}u|u| \tag{4}$$

- *Sway terms*

$$\begin{aligned}\tau^b_{Yhyd} &= Y_{\dot{v}}\dot{v} + Y_{\dot{r}}\dot{r} + Y_{\dot{p}}\dot{p} + Y_{|u|v}|u|v + Y_{ur}ur + Y_{|v|v}|v|v + Y_{|v|r}|v|r \\ &+Y_{|r|v}|r|v + Y_{\phi|uv|}\phi|uv| + Y_{\phi|ur|}\phi|ur| + Y_{\phi uu}\phi u^2\end{aligned} \tag{5}$$

- *Roll terms*

$$\begin{aligned}\tau^b_{Khyd} &= K_{\dot{v}}\dot{v} - K_{\dot{p}}\dot{p} + K_{|u|v}|u|v + K_{ur}ur + K_{|v|v}|v|v + K_{|v|r}|v|r + K_{|r|v}|r|v \\ &+K_{\phi|uv|}\phi|uv| + K_{\phi|ur|}\phi|ur| + K_{\phi|uu|}\phi u^2 + K_{|u|p}|u|p + K_{p|p|}p|p| + K_p p \\ &-K_{\phi\phi\phi}\phi^3 + \rho g \nabla GMt\phi\end{aligned} \tag{6}$$

- *Yaw terms*

$$\begin{aligned}\tau^b_{Nhyd} &= N_{\dot{v}}\dot{v} + N_{\dot{r}}\dot{r} + N_{|u|v}|u|v + N_{ur}ur + N_{|v|v}|v|v + N_{|v|r}|v|r + N_{|r|v}|r|v \\ &+N_{\phi|uv|}\phi|uv| + N_{\phi u|r|}\phi u|r| + N_{|p|p}|p|p + N_{|u|p}|u|p + N_{\phi u|u|}\phi u|u|\end{aligned} \tag{7}$$

Note that $\dot{\psi} = r$ and $\dot{\phi} = p$.

B. Propulsion Forces

The dynamics of the propulsion system are not included in the model as in [24]. Instead of that, it is assumed that the propellers deliver a constant thrust T that compensates the resistance on calm water:

$$T = -X_{u|u|}u^2_{nom} \tag{8}$$

where u_{nom} is the service speed. The resultant propulsion forces vector is:

$$\tau_p = [T,\ 0,\ 0,\ 0]^T \tag{9}$$

Consequently, the rudder′s and fin′s motion induce drag forces that contribute to slow down the vessel.

C. Control Forces: Rudder

The vessel under study in here is equipped with two rudders which together with the commanding machinery constitute the actuators of the system. In order to obtain the expression of the control forces, some other concepts need to be introduced first.

Hydrofoil lift and drag forces [27], are given by the following expressions:

$$L = 1/2\rho V_f^2 A_f \bar{C}_L \alpha_e \tag{10}$$

$$D = 1/2\rho V_f^2 A_f (C_{D0} + \frac{(\bar{C}_L \alpha_e)^2}{0.9\pi a}) \tag{11}$$

where V_f is the local velocity at the foil, A_f is the area of the foil, α_e is the effective angle of attack in radians, and a is the effective aspect ratio. We can use the following linear approximation to represent the lift coefficient:

$$\bar{C}_L = \frac{\partial C_L}{\partial \alpha_e}|_{\alpha_e=0} \tag{12}$$

Once the stall angle of the hydrofoils is reached, the lift saturates in value. In order to calculate the lift of the rudder, the effective angle of attack, α_e, is approximated by the mechanical angle of the rudder: $\alpha_e \approx \delta_c$, and the local flow velocity at the rudder is considered to be equal to the vessel's total horizontal speed, $V_f = \sqrt{u^2 + v^2}$. Then, a global correction for the lift and drag can be applied [28]:

$$\Delta L = T\left[1 + \frac{1}{1 + C_{Th}} sin(\alpha_e)\right] \tag{13}$$

$$\Delta D = T\left[1 + \frac{1}{1 + C_{Th}} (1 - cos\,(\alpha_e))\right] \tag{14}$$

where T is the propeller′s thrust, and C_{Th} is the propeller′s loading coefficient given by:

$$C_{Th} = \frac{2T}{\rho V_f^2 A_p} \tag{15}$$

in which A_p is the propeller′s disc area.

The control forces, τ_c, generated by the rudder in the b-frame are:

$$\tau_c \approx [-D,\ L,\ z_{CP}^b L,\ x_{CP}^b L]^T \tag{16}$$

where x_{CP}^b and z_{CP}^b are the coordinates of the center of pressure of the rudder (CP) with respect to the b-frame. The CP is assumed to be located at the rudder stock and in the middle of the rudder span.

The hydraulic machinery moving the rudder is implemented in this work following the model of [29] that considers both a maximum rudder angle and rate. When working in the unsaturated zone, the rudder′s dynamics can be represented by a first order system of the form:

$$\dot{\delta}(t) = \frac{1}{T_m}\left[\delta_c(t) - \delta(t)\right] \tag{17}$$

where $\delta(t)$ is the actual rudder angle, $\delta_c(t)$ is the commanded rudder angle and T_m is the time constant of the hydraulic machinery.

D. Kinematics

The kinematics cover the geometrical aspects of the vessel′s displacement without considering mass and forces. The position of the ship is obtained by performing a transformation between the body-fixed ($b - frame$) linear velocities and the time derivative of the positions in the ($n - frame$), see figure 1. This can be expressed for a 6 DOF manoeuvring model as:

$$\begin{bmatrix} \dot{x}_n \\ \dot{y}_n \\ \dot{z}_n \end{bmatrix} = R_b^n \begin{bmatrix} u \\ v \\ w \end{bmatrix}, \tag{18}$$

where u is the surge speed, v is the sway speed and w is the heave speed.
The linear-velocity transformation matrix R_b^n is [30], [31]:

$$R_b^n = \begin{bmatrix} c\psi c\theta & -s\psi c\phi + c\psi s\theta s\phi & s\psi s\phi + c\psi c\phi s\theta \\ s\psi c\theta & c\psi c\phi c\phi + s\phi s\theta s\psi & -c\psi s\phi + s\psi c\phi s\theta \\ -s\theta & c\theta s\phi & c\theta s\phi \end{bmatrix}, \tag{19}$$

where ψ is the yaw angle, ϕ is the roll angle, θ is the pitch angle, $s \equiv sin(\cdot)$ and $c \equiv cos(\cdot)$.
For the case of the 4 DOF manoeuvring model of this work, the movement in the z axe is not considered and $\theta = 0$, then, by taking this into account, equations (18) and (19) are simplified as follows:

$$\begin{aligned} \dot{x}_n &= u \cdot cos(\psi) - v \cdot sin(\psi)cos(\phi) \\ \dot{y}_n &= u \cdot sin(\psi) + v \cdot cos(\psi)cos(\phi) \end{aligned} \tag{20}$$

Note that all the variables were previously defined in table I .

III. ITERATION TECHNIQUE FOR NONLINEAR SYSTEMS

This section revises the implementation and convergence properties of a recently introduced technique for solving nonlinear dynamical systems. In this methodology, the original nonlinear problem is replaced by a sequence of linear time varying systems whose solutions converge in the space of continuous functions to the solution of the nonlinear system under a mild Lipschitz condition [17]. This section contains the basis on how this technique is implemented and its convergence theorem.

Any nonlinear system given on the form:

$$\dot{x}(t) = f[x(t)] = A[x(t)]x(t) + B[x(t)]u_c(t), \quad x(0) = x_0 \in \mathbb{R}^n. \tag{21}$$

where $A[x(t)] \in \mathbb{R}^{n\text{x}n}$ is locally Lipschitz, can be approximated by a sequence of linear time varying equations where the vector of states $x(t) \in \mathbb{R}^n$, inside the matrices $A[x(t)]$ and $B[x(t)]$ are substituted at each iteration "i" by the states obtained in the previous iteration $x^{(i-1)}(t)$:

$$\begin{aligned} \dot{x}^{(1)}(t) &= A[x(0)]x^{(1)}(t) + B[x(0)]u_c^{(1)}(t), \quad x^{(1)}(0) = x(0) \\ &\vdots \\ \dot{x}^{(i)}(t) &= A[x^{(i-1)}(t)]x^{(i)}(t) + B[x^{(i-1)}(t)]u_c^{(i)}(t), \quad x^{(i)}(0) = x(0) \end{aligned} \tag{22}$$

for $i \geq 1$ and $\forall t \in [0, \tau]$. The solutions of this sequence of linear time varying equations, $x^{(i)}(t)$ converge to the solution of the nonlinear system $x(t)$ given in (21):

$$Lim_{i\to\infty} \left[x^{(i)}(t)\right] \to x(t) \tag{23}$$

The convergence of this sequence is stated in the following theorem:

Theorem I: Suppose that the nonlinear equation (21) has a unique solution on the time interval $t \in [0, \tau]$ *denoted by* $x(t)$ *and assume that the system's matrix* $A[x(t)] : R^n \to R^n$ *is locally Lipschitz. Then, the sequence of solutions defined in (23) converges uniformly on* $t \in [0, \tau]$ *to the solution* $x(t)$.

The convergence proof of *Theorem I* can be found in [17] where global convergence is extended to time intervals $t \in [0, \infty]$, the reader is referred to this cite for a detailed mathematical derivation of the proof.

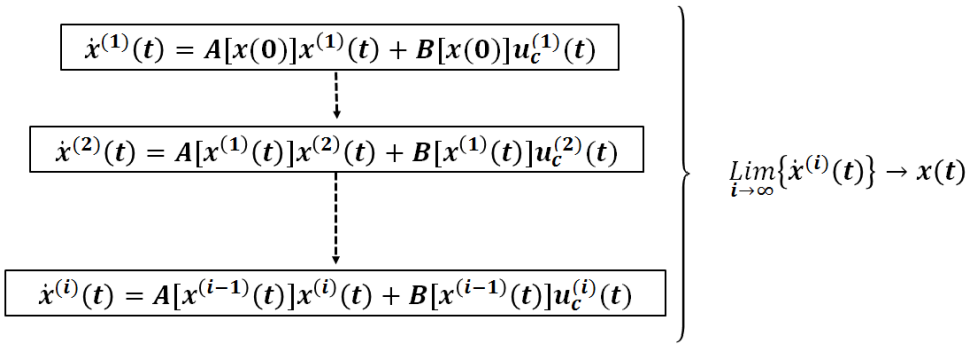

Fig. 2. The sequence of linear time varying solutions defined in (23) converges uniformly on $t \in [0, \tau]$ to the solution $x(t)$ of the nonlinear problem.

The application of this technique provides an accurate representation of the nonlinear solution after just a few iterations. Nonlinear systems of the form (21), satisfying the local Lipschitz requirement can be now approached by classic linear methods. This is a very mild assumption since it is an already assumed condition for the uniqueness of solution in *Theorem* I.

IV. Approximation to the vessel's nonlinear equations

In this section the authors show how to apply the iteration technique presented in section III to approximate the vessel's nonlinear model given in section II for the particular case of a full scale coastal patrol. The set of parameters and the main characteristics of the coastal patrol are included in Appendix A. The coastal patrol is equipped with two rudders and its service speed is $u_{nom} = 15$ knots $(7.71m/s)$. The simulations were carried out using Matlab/Simulink and the GNC toolbox [32]. The simulation time was $t_f = 200$ secs and the integration step size was set to be $h = 0.1$. As a rule of thumb, the sampling period h is chosen to be in the range of 20-40 samples within the rise time of the fastest degree of freedom.

The equations of motion of this system, (2)-(20), are highly nonlinear and can be written on the form:

$$\dot{x}(t) = A[x(t)]x(t) + B[x(t)]u_c(t), \quad x(0) = x_0 \in \mathbb{R}^9. \tag{24}$$

where the systems matrix $A[x(t)] \in \mathbb{R}^{9x9}$, $B[x(t)] \in \mathbb{R}^{9x2}$, $u_c(t)$ is the control signal and $x(t)$ is the state vector, $x(t) = [u\ v\ p\ r\ \phi\ \psi\ \delta\ x\ y]^T$. u is the surge (longitudinal speed), v is the sway,

this is the lateral speed, p is the angular speed of roll, r is the angular speed on yaw, ϕ is the angular displacement in roll, ψ is the angular displacement in yaw, δ is the rudder displacement for direction management purposes and x_n, y_n are the corresponding coordinates for longitudinal and lateral positions expressed in the n-frame.

A standard 20°-20° zig-zag manoeuvre (see [27]) is simulated, the reason for choosing such a large amplitude is to excite the vessel′s high nonlinear dynamics and to show the good fit of the iteration technique to the nonlinear original system. The control vector to carry out this manoeuvre is $u_c(t) = [\delta_c \ T]^T$, where T was previously defined in (8) and δ_c is the rudder′s deflection that must follow the zig-zag manoeuvre phases as shown in figure 3. Despite there is no control methodology design, the zig-zag manoeuvre is in closed loop as the actual value of $\psi(t)$ is measured and until it reaches a determined value the rudder does not change from starboard to port or viceversa (see 2^{nd}, 3^{rd}, 4^{th}, and 5^{th} phase points where the rudder angle of deflection is changed in figure 3). The zig-zag manoeuvre should be completed with at least five phases.

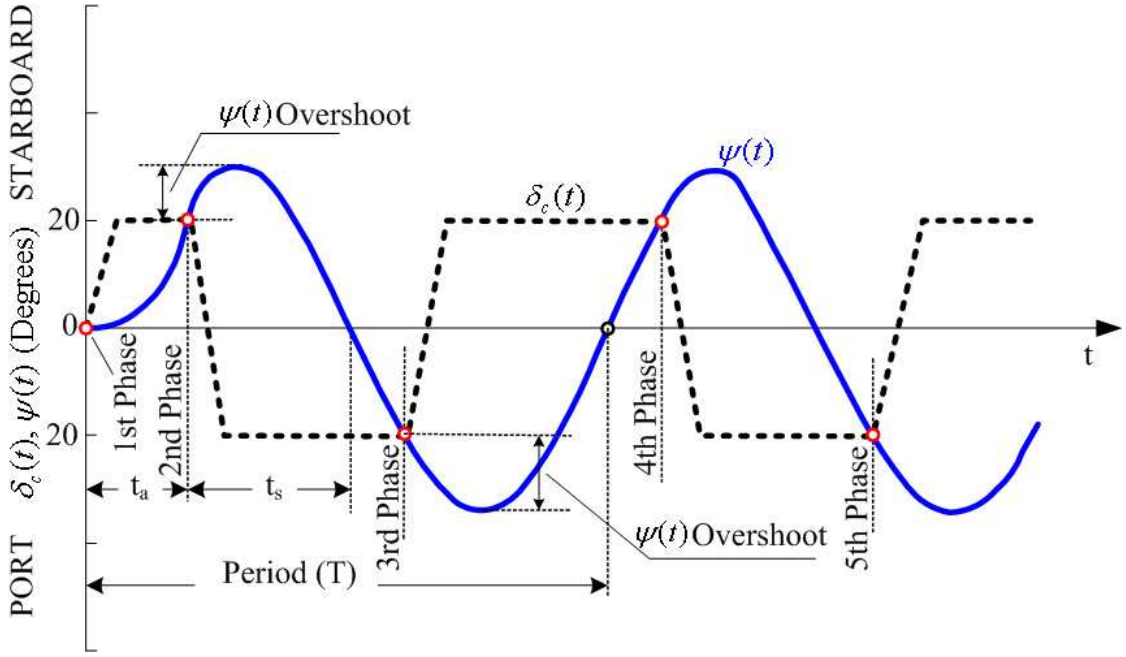

Fig. 3. 20°-20° zig-zag manoeuvre phases and corresponding values of the heading angle $\psi(t)$ represented in solid blue line and the rudder′s deflection $\delta_c(t)$ represented by dashed black line.

The initial conditions, $x_0 = [u_{nom} \ 0 \ 0 \ 0 \ 0 \ 0 \ 0 \ 0]^T$, substitute the states on the first approximated

linear system′s matrices, $A[x_0]$, $B[x_0]$ and, subsequently, the iteration technique results in a sequence of linear time varying (LTV) systems where 20 iterations were needed to approach the original nonlinear system.

Figures (4)-(7) show the time history of various states during the 20°-20° zig zag manoeuvre for some of the iterations and as well the evolution in time of the states in the nonlinear case (red line), this is done in order to illustrate the convergence of this method. It is shown how the 20^{th} solution is a good representation of the nonlinear system solution, also the 40^{th} solution is shown in order to demonstrate the convergence of the states. After the 20^{th} iterated solution, $x^{(20)}(t)$, the convergence to the nonlinear solution $x(t)$ is clear and also it is shown how the consequent iterations, i.e., $x^{(40)}(t)$ show little variation with respect to it, this is, $\left\|x^{(40)}(t) - x^{(20)}(t)\right\| \to 0$ when $t \to \infty$.

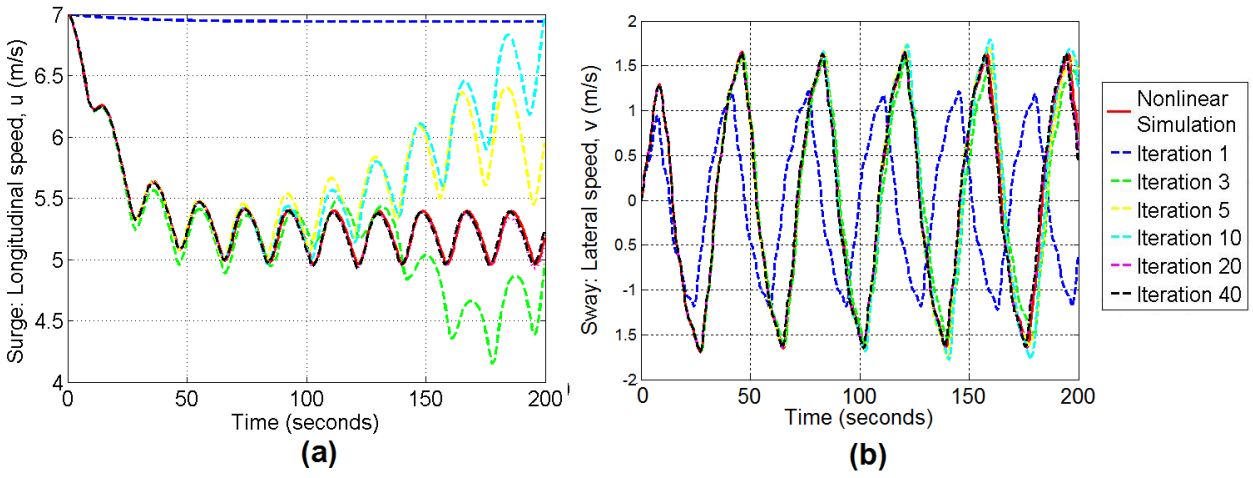

Fig. 4. Convergence of $u(t)$ and $v(t)$ states on a 20°-20° zig-zag manoeuvre. Red line represents the movement of the original nonlinear system. The pink line represents the 20^{th} iterated linear time varying approximation and the black line is the 40^{th} iteration.

Figure 7.b shows the vessel′s position on the plane (x_n, y_n) along this manoeuvre; it is clear to see how the 20^{th} iteration (pink line) gives an accurate approximation to the behavior of the original nonlinear system (red line). From the previous figures, it is clear to conclude that when the iteration technique is implemented, after a short number of iterations, the original nonlinear expression for the vessel′s dynamics gets a good representation by the last of the linear approximations, 20 in this particular case.

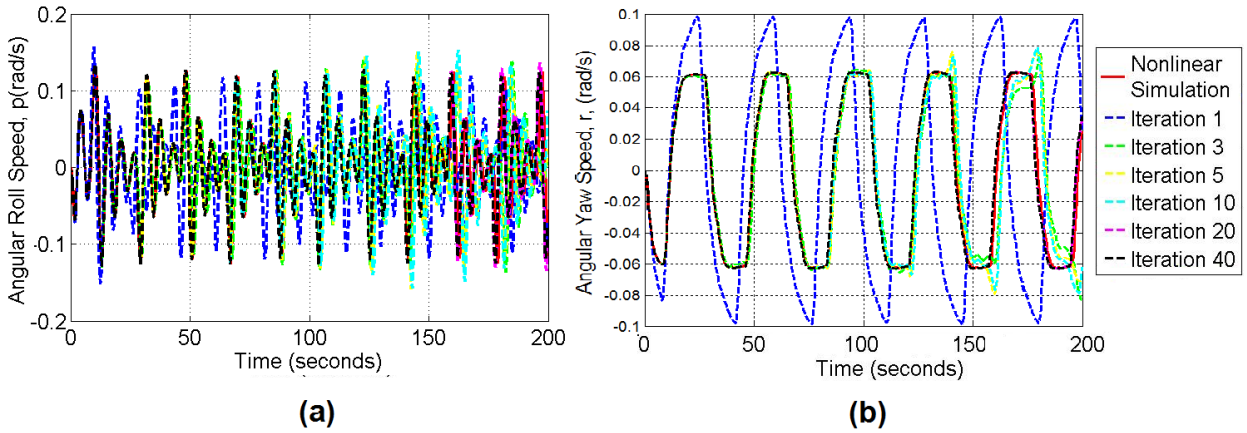

Fig. 5. Convergence of $p(t)$ and $r(t)$ states on a 20°-20° zig-zag manoeuvre. Red line represents the movement of the original nonlinear system. The pink line represents the 20^{th} iterated linear time varying approximation and the black line is the 40^{th} iteration.

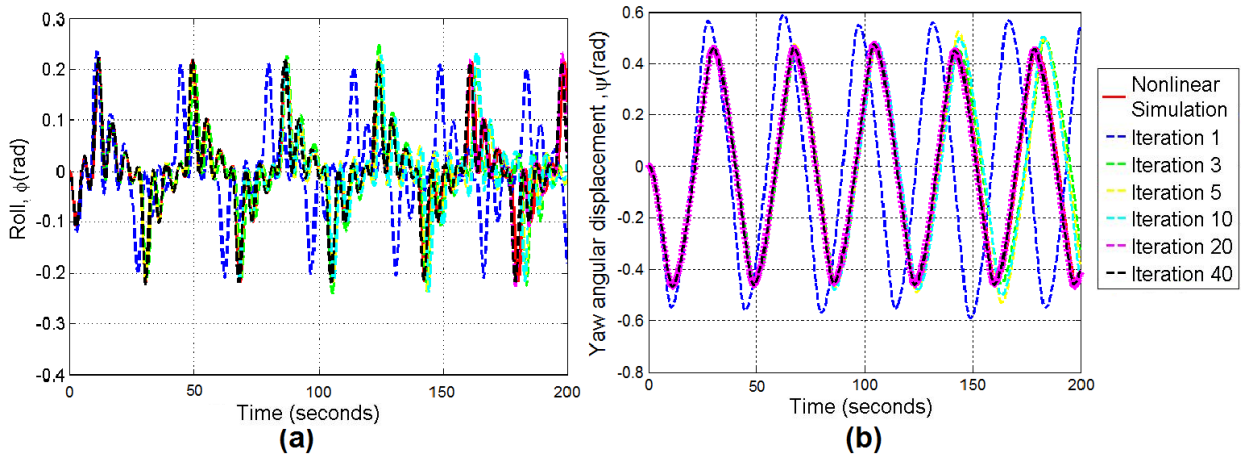

Fig. 6. Convergence of $\phi(t)$ and $\psi(t)$ states on a 20°-20° zig-zag manoeuvre. Red line represents the movement of the original nonlinear system. The pink line represents the 20^{th} iterated linear time varying approximation and the black line is the 40^{th} iteration.

V. Control of the Vessel's Nonlinear Dynamics

A. Controller design

An automatic pilot must fulfil two functions: course-keeping and change of course. In the first case, the control objective is to maintain the trajectory of the vessel following a desired constant heading, ψ_d. In the second case, the objective is to perform heading changes without introducing

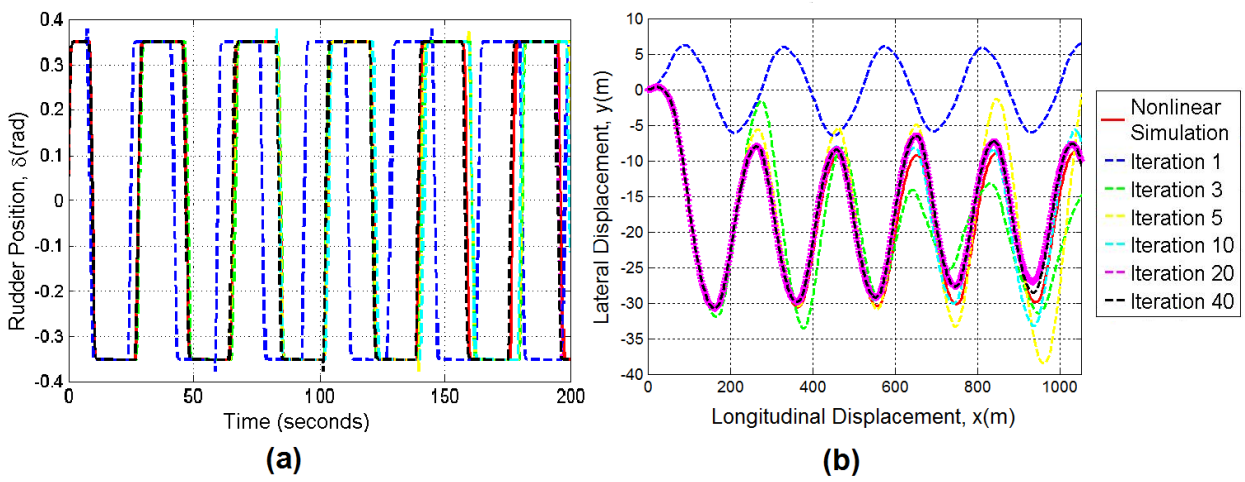

Fig. 7. (a) Convergence of $\delta(t)$ state on a 20°-20° zig-zag manoeuvre. Red line represents the movement of the original nonlinear system. The pink line represents the 20^{th} iterated linear time varying approximation and the black line is the 40^{th} iteration. (b) Vessel′s position on the plane (x_n, y_n) along this manoeuvre

large response oscillations and within a minimum time. In both cases, the adequate functioning of the system must be independent from the disturbances produced by existing external factors such as wind, waves and currents.

The heading trajectory followed by the vessel, $\psi(t)$, can be obtained by means of a second order reference model:

$$\ddot{\psi}(t) + 2\zeta w_n \dot{\psi}(t) + w_n^2 \psi(t) = w_n^2 \psi_d \tag{25}$$

where w_n is the natural frequency and ζ is the desired damping ratio of the closed loop system. ζ is typically chosen to lie within the interval values $(0.8 \leq \zeta \leq 1)$ in order to account for security issues [33]. In restricted waters and for collision avoidance, the course-changing manoeuvre should have a clear start, in order to warn nearby ships of the intention of the manoeuvre and, for that reason, that manoeuvre should preferably be completed with no overshoot.

The following PID control schema is conventionally used for the heading control implementation:

$$U_c(s) = \frac{\delta_c}{E}(s) = \left[k_p + \frac{k_i}{s} + \frac{k_d s}{\alpha T_d s + 1} \right] \tag{26}$$

where $k_d = T_d k_p$ and $k_i = k_p / T_i$ being T_d the derivative time, T_i the integral time, $\delta_c(s)$ the Laplace transform of the rudder position and $E(s)$ the Laplace transform of the error, $e(t) = \psi_d - \psi(t)$ and $U_c(s)$ is the Laplace transform of the control signal, $u_c(t, \theta_c)$. The $\psi(t)$ vector is

extracted from the states, being $x(t) = [u\ v\ p\ r\ \phi\ \psi\ \delta\ x\ y]^T$ and $x_{(6)}(t) = \psi(t)$.

The noise levels of the onboard standard instrumentation may cause derivative model noise amplification problems. The PID schema (26), in which the derivative action is filtered by a first order system $\frac{1}{\alpha T_d s+1}$, avoids this problem of noise amplification.

It is highly likely that the rudder's deflection angle and rate saturations provoque the windup phenomenon (see [34] for more details) when PID methodology is applied. This is, the PID integral term, $(\frac{k_i}{s})$, may become large and as a consequence, the heading response may show high levels of oscillation. There exist several anti-windup schemes in the literature (see [34] and references therein), but instead of applying one of them, this would make the designed controller more complex, a simpler method is chosen: a modified control structure such as the following first order network controller is proposed, note that the integral action has been omitted:

$$U_c(s) = \frac{\delta_c}{E}(s) = K\left[\frac{s+z}{s+p}\right] \tag{27}$$

where $K > 0$ and $p > z$.

The expression (27) represents a lead compensation controller [35] that has a zero located nearer to the s-plane origin than the pole. This dominant zero improves the stability of the system, which is desirable in order to satisfy the objective of obtaining a heading response without overshoot.

Note that equations (26) and (27) become equal to each other if the integral term $K_p/(T_i s)$ is zero, being equivalent to a PD controller transfer function.

B. Tuning the controller

The tuning task is performed by following the schema on figure 8, in which the optimization algorithm takes data from the output (vessel′s heading angle $\psi(t)$) and from the input (desired heading ψ_d). In the selection of the optimization method the aims of the heading control were taken into account: To minimize both the response′s overshoot and the settling time without steady state error. For these reasons, the authors chose the minimax optimization technique, as it minimizes the maximum value of the output. In this way, when the maximum value of the output is reduced, the heading′s overshoot is minimized too.

The application of the minimax problem to the heading control, consist on minimizing the maximum value of the output, $\psi(t)$, over the simulation time interval $[t_0, t_f]$. The following

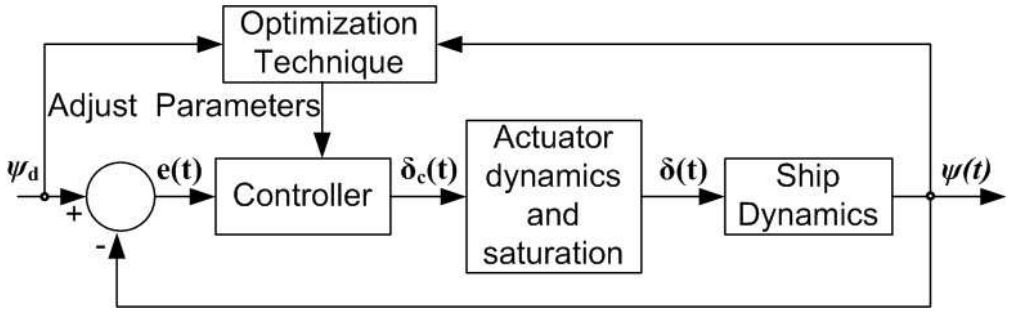

Fig. 8. Closeloop diagram for the optimization process.

constrain is imposed such that $\psi(t)$ is always less or equal than the constant input value ψ_d,

$$\psi(t) \leq \psi_d, \quad t_r \leq t \leq t_f \tag{28}$$

being t_r the rise time of the system. By imposing this restriction, a flat response with no overshoot and no stationary error is expected. The value of t_r is determined based on a prior knowledge of the system response. Then, the Minimax problem is applied [36], [37]:

$$\min_{\theta_c^{(i)}} \max_{j} \{\psi_j(\theta_c^{(i)})\} \equiv \begin{cases} \psi(t) \leq \psi_d, \quad t_r \leq t \leq t_f \\ lb \leq \theta_c^{(i)} \leq ub \end{cases}$$

where $\psi(t)$ is the heading angle, $\theta_c^{(i)}$ are the controller's parameters for the corresponding i^{th} linear time varying approximation to be optimized , lb is the lower bound of the parameters, ub is the upper bound of the parameters and the subindex j represents one set of multivariable functions.

C. Implementation Procedure

Based on the theory previously presented, the heading control implementation process can be summarized according to the following steps:

Initialization

- Set initial values for the constants and variables involved in the process: $lb, ub, x(0), \theta_c^{(0)}, t_0, t_f, t_r, \psi_d, h, tol_x, tol_{\theta_c}$.

Step (1)

- The first step to solve system (31) is to approximate it by solving the following linear time invariant system:
  $\dot{x}^{(1)}(t) = A[x_0]x^{(1)}(t) + B[x_0]u_c^{(1)}(t, \theta_c^{(1)}), \quad x^{(1)}(0) = x_0.$
  This system represents a linear model and it differs from the nonlinear behaviour, not being a good representation; that is the reason why the heading control is not optimized at this step, then we made $\theta_c^{(1)} = \theta_c^{(0)}$.

Step (2)

1) Optimize the heading control loop:

$$\min_{\theta_c^{(2)}} \max_{j} \{\psi_j(\theta_c^{(2)})\} \equiv \begin{cases} \psi(t) \leq \psi_d, \quad t_r \leq t \leq t_f \\ lb \leq \theta_c^{(2)} \leq ub \end{cases}$$

   for $j = 1, 2, \ldots t_f/h$. The optimization stops when $\|\theta_c^{(2)} - \theta_c^{(1)}\| < tol_{\theta_c}$ is true.

2) With the obtained parameters $\theta_c^{(2)}$, the following linear time varying system is solved for $x^{(2)}(t)$ by using the designed control action $u_c^{(2)}(t, \theta_c^{(2)})$:
   $\dot{x}^{(2)}(t) = A[x^{(1)}]x^{(2)}(t) + B[x^{(1)}]u_c^{(2)}(t, \theta_c^{(2)}), \quad x^{(2)}(0) = x(0).$
   If $\|x^{(2)} - x^{(1)}\| < tol_x$ is true the algorithm stops here, if not go to step 3.

$$\vdots$$

Step (i)

1) Optimize the heading control loop by:

$$\min_{\theta_c^{(i)}} \max_{j} \{\psi_j(\theta_c^{(i)})\} \equiv \begin{cases} \psi(t) \leq \psi_d, \quad t_r \leq t \leq t_f \\ lb \leq \theta_c^{(i)} \leq ub \end{cases}$$

   for $j = 1, 2, \ldots t_f/h$. The optimization stops when $\|\theta_c^{(i)} - \theta_c^{(i-1)}\| < tol_{\theta_c}$ is true.

2) With the obtained parameters $\theta_c^{(i)}$, the next step is to solve the following linear time varying system:
   $\dot{x}^{(i)}(t) = A[x^{(i-1)}]x^{(i)}(t) + B[x^{(i-1)}]u_c^{(i)}(t, \theta_c^{(i)}), \quad x^{(i)}(0) = x(0).$
   If $\|x^{(i)} - x^{(i-1)}\| < tol_x$ is true the algorithm stops here, if not go to step $i + 1$.

Note that in the optimization process, in order to obtain the set of functions $\{\psi_j(\theta_c^{(i)})\}$ it is necessary to solve the corresponding linear time varying approximation:

$$\dot{x}^{(i)}(t) = A[x^{(i-1)}]x^{(i)}(t) + B[x^{(i-1)}]u_c^{(i)}(t, \theta_c^{(i)}), \quad x^{(i)}(0) = x(0) \tag{30}$$

to obtain $x^{(i)}$, as much as needed by the optimization algorithm. The control output $u_c^{(i)}(t, \theta_c^{(i)})$ at each iteration is given by the control structure defined in section V-A.

D. Iteration technique approximation for control purposes

In this section, the methodology previously introduced is applied to the case of heading control of the vessel model. The equations of motion of this system are highly nonlinear and can be written on the form:

$$\dot{x}(t) = A[x(t)]x(t) + B[x(t)]u_c(t, \theta_c), \quad x(0) = x_0 \in \mathbb{R}^n. \tag{31}$$

where $A[x(t)] \in \mathbb{R}^{nxn}$, $B[x(t)] \in \mathbb{R}^{nxm}$, $x(t)$ is the state′s vector and the control $u_c(t, \theta_c)$ is designed by using the methodology presented in section V-A. The system (31) can be approximated by the following sequence of linear time varying systems:

$$\begin{aligned} \dot{x}^{(1)}(t) &= A[x(0)]x^{(1)}(t) + B[x(0)]u_c^{(1)}(t, \theta_c^{(1)}), \quad x^{(1)}(0) = x(0) \\ &\vdots \\ \dot{x}^{(i)}(t) &= A[x^{(i-1)}(t)]x^{(i)}(t) + B[x^{(i-1)}]u_c^{(i)}(t, \theta_c^{(i)}), \quad x^{(i)}(0) = x(0) \end{aligned} \tag{32}$$

For each of these "i" linear time varying iterations, a control action signal $u_c^{(i)}(t, \theta_c))$ is designed. Once last iteration is obtained, the sequence of solutions converges to the nonlinear solution, $Lim_{i\to\infty}\left[x^{(i)}(t)\right] \rightarrow x(t)$. The last designed control signal will be applied to the original nonlinear problem, achieving control of the states:

$$\dot{x}(t) = A[x(t)]x(t) + B[x(t)]u_c^{(i)}(t, \theta_c^{(i)}), \quad x(0) = x_0 \in \mathbb{R}^n. \tag{33}$$

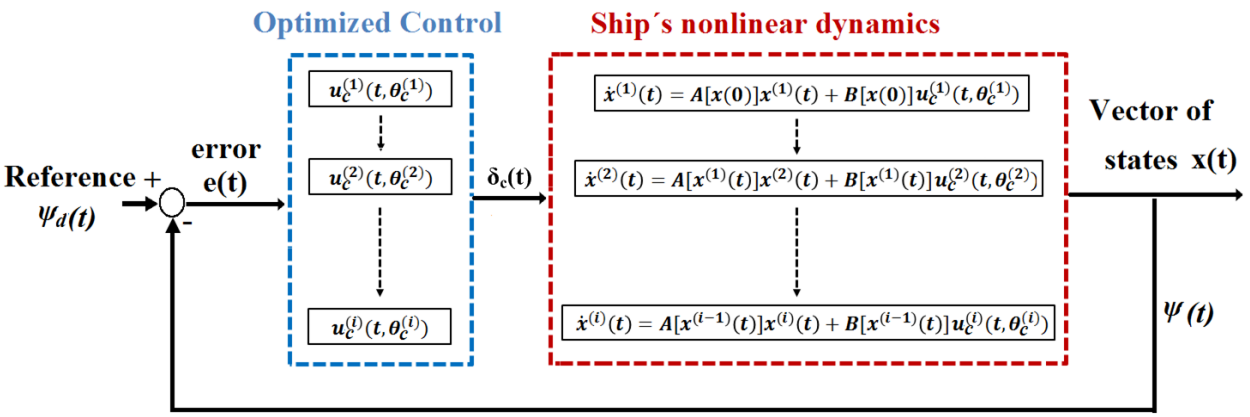

Fig. 9. Diagram of the optimization algorithm connected to the iteration technique.

VI. Simulations and Results

The simulation scenario is based on the coastal patrol full-scale vessel data used in section III. A course keeping manoeuvre of ψ_d=20° degrees will validate and test the iterative controller design implemented following the steps given in section V-C. The manoeuvre should be completed satisfying the objectives stated in section V-A.

The vessel′s model defined in section II is rearranged on the form $\dot{x} = A(x)x(t) + B(x)u_c(t,\theta_c)$ where $x(t,\theta_c) = [u\ v\ p\ r\ \phi\ \psi\ \delta\ x\ y]^T$ and the control vector is $u_c(t,\theta_c) = [\delta_c\ T]^T$. The initial conditions are taken from [22] as: $x_0 = [u_{nom}\ 0\ 0\ 0\ 0\ 0\ 0\ 0\ 0]^T$.

In previous results for the 20° course-keeping manoeuvre case, a PID controller (26) was applied and a high value of T_i was obtained by the optimization method. As explained in section V-A, the optimization technique applied for the tuning, in an attempt to reduce the oscillation caused by the integral windup problem, provides a high value of T_i and therefore reduces to the minimum the influence of the integral term. This suggest that the contribution of the integral term k_i/s in the PID controller (26) (being $k_i = k_p/Ti$) can be neglected. For all of this reasons, a lead compensation controller (27) without integral action is used instead. The constrains of the controller parameters were set to $lb = 0$ and $ub = \infty$, in order to avoid unstable controller behaviour. The lead compensation controller initial parameters were selected taking into account that this type of controller must have a dominant zero near to the s-plane origin.

Figures 10 and 11 show the results for a course keeping 20° (0.349 rad) manoeuvre for each

iteration "i". After the 5^{th} iteration, the algorithm converges, the corresponding control parameters θ_c and the heading response $\psi(t)$ remain almost unchanged. The zoom made for the yaw variable $\psi(t)$ on the top part of Figure 10 for the iterations 5-8 shows that the difference between iterations i and $i-1$, is within the order of $\frac{1}{100}$ of degree, illustrating the convergence properties of the presented algorithm. Figures 10 and 11 clearly show an accurate approximation for the 5^{th} iteration to the nonlinear model (compare iteration 5 with the simulated data generated with the original nonlinear system and the controller parameters $\theta_c^{(5)}$). At this stage, (i=5), the overshoot is reduced in the heading response $\psi(t)$ and the settling time is reduced with respect to the previous iterations. Furthermore, the steady state error ($e(t) = \psi_d - \psi(t)$) converges to zero after only 30 seconds. The bottom part of figure 10 shows the actuator's displacement, $\delta(t)$, which represents the actual value of the rudder's angle of deflection. There is saturation present in the actuator for the $5th$ iteration, but with the selected lead compensation controller the windup problem is avoided obtaining a response without overshoot. The lead compensation controller is a simpler solution that an anti-windup scheme for the PID controller.

VII. Conclusions

In this work, the authors proposed a control strategy based on an optimized lead compensation controller methodology combined with an iteration technique based on linear time varying approximations to approach the nonlinear dynamics of a ship. The theory here presented has been implemented in Matlab/Simulink and applied to the particular example of a full scale coastal patrol vessel under two different scenarios: firstly, a standard 20°-20°zig-zag manoeuvre is considered in order to show the convergence of the iteration methodology presented in the theory and secondly, a 20° course-keeping manoeuvre is presented to show the accuracy of the tracking capabilities of the designed controller when applied to the last of iterated linear time varying systems.

On the first case, the results show that the approximation to the vessel's nonlinear dynamical equations in the $20° - 20°$ zig-zag manoeuvre is a good approximation after only a few number of iterations, 20 in this case. By generating this sequence of linear time varying equations that approximate the original nonlinear dynamics, now linear control techniques can be applied to the last of these iterations. This is a good advantage since linear control methods are usually simpler and computationally cheaper to implement.

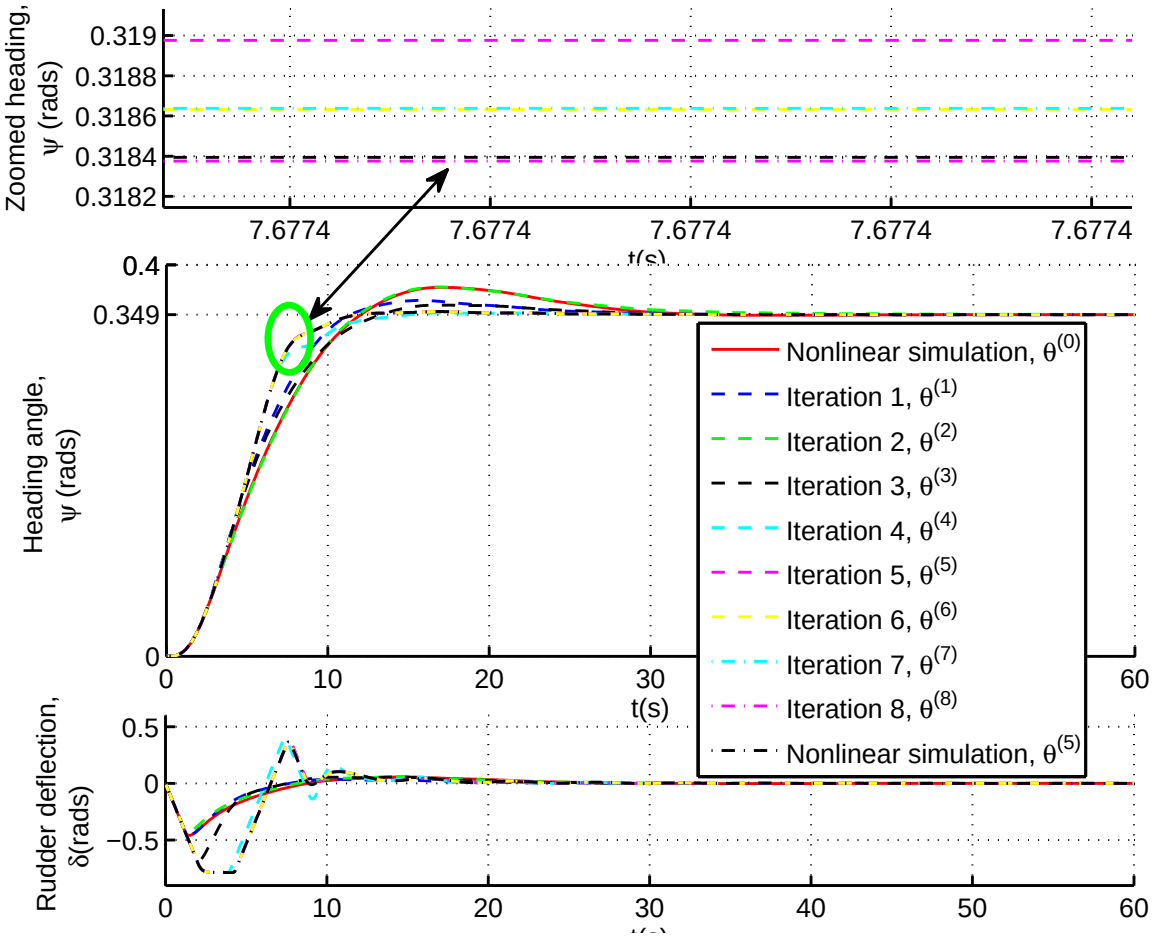

Fig. 10. Convergence results of the controlled variable $\psi(t)$ and the actuator′s variable, the rudder deflection, $\delta(t)$, for the coastal patrol vessel on a course keeping 20° manoeuvre.

On the other hand, for the 20° course-keeping manoeuvre, the proposed control strategy and reference tracking methodology is tested. A high value of T_i obtained with the proposed control strategy in preliminar results, indicates that the rudder′s saturation provoques the integral windup problem when PID control is applied. Therefore, it is advisable to use a controller without integral term such as the lead compensation controller. The presented results with the lead compensation controller meet the stated objectives in the heading response: the elimination of the existing overshoot, the reduction of the settling time and the elimination of the steady state error. In addition to this, the lead compensation controller constitutes a simpler solution than an anti-windup scheme for a PID controller.

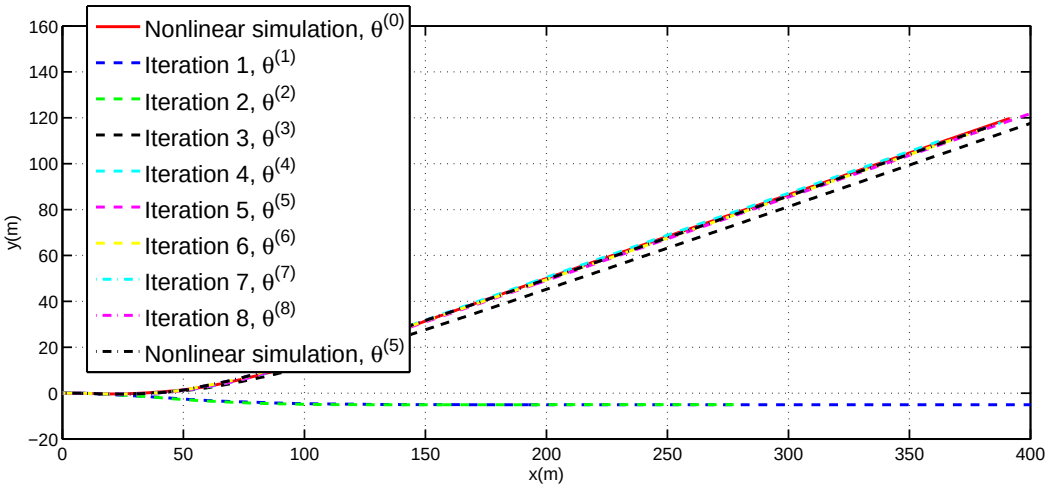

Fig. 11. Position convergence results for the coastal patrol vessel for a course keeping 20° manoeuvre.

The authors are currently investigating further within this area. The control strategy here proposed will be extended to the multivariable control case in order to develop a trajectory control system.

APPENDIX

For the Coastal patrol [22], [24] the main hull data and load condition are given in table II and figure 12. The hydrodynamic coefficients of the manoeuvring model are included in table V and the data corresponding to the propulsion system are in tables IV and III. The vessel is equipped with two rudders.

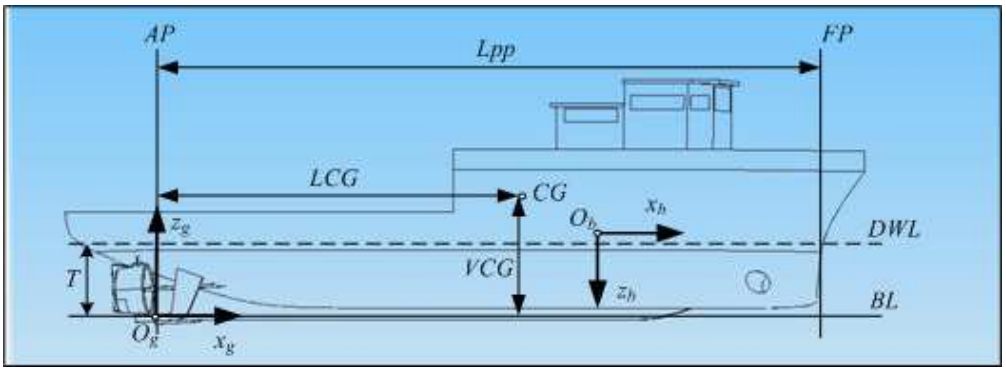

Fig. 12. Main particulars and reference frames.

Note that o_g is the geometrical coordinate origin, see [22] for more details.

TABLE II

PRINCIPAL SHIP DIMENSIONS AND LOAD CONDITION.

Quantity	**Symbol**	**Full Load**
Length between perpendiculars	L_{pp}	51.5 m
Beam	B	8.6m
Mass	m	$364.78\times10^3 Kg$
Centre of gravity	CG	-
Lateral Centre of Gravity from AP	LCG	19.82 m
Vertical Centre of Gravity from MBL	VCG	3.36 m
Stern perpendicular	AP	-
Bow perpendicular	FP	-
Draft at $L_{pp}/2$	T	2.29 m
Design water line	DWL	-
Base line	BL	-
Displacement	∇	355.88 m^3
Nominal speed (service speed)	u_{nom}	15 kt
Inertia roll moment	I_{xx}	$3.4263\times10^3 Kgm^2$
Inertia yaw moment z	I_{zz}	$3.3818 \times 10^3 Kgm^2$
Distance in the x axes from CG to O_b	x_G	-3.38 m
Distance in the z axes from CG to O_b	z_G	-1.06 m
Transverse Metacentric Height	GMt	3.34 m

TABLE III

FREE STREAM DATA FOR RUDDER AND FIN PROFILES (SEE [27]).

Profile Tip a(eff)	$\frac{\partial C_L}{\partial \alpha_e}$	C_{Lmax}	C_{D0}	α_{stall}
NACA15 SQUARE 3	0.054	1.25	0.0065	23
NACA15 SQUARE 2	0.046	1.33	0.0065	28.8

ACKNOWLEDGMENTS

This paper has been partially supported by the Spanish Ministry of Defense, matching program-1003211003100 and by the MICINN:DPI2011-27990.

TABLE IV

RUDDER DATA.

Quantity	**Symbol**	**Measure**
Area	A_f	$2{\times}1.5m^2$
Span	sp	1.5 m
Mean cord	$\bar{c}$	1 m
Eff. aspect ratio	a	3
Max. angle	δ_{max}	40 deg
Max. rate	$\dot{\delta}_{max}$	20 deg/s
Prop. band	δ_{pb}	4 deg
Vert. Dist. $O_b - CP$	z^b_{CP}	2.61 m
Horiz. Dist. $O_b - CP$	x^b_{CP}	1.5 m

TABLE V

HYDRODYNAMIC COEFFICIENTS FOR THE MANOEUVRING MODEL.

X-Coefficients	Y-Coefficients	K-Coefficients	N-Coefficients
$X_{\dot{u}}$=-17400	$Y_{\dot{v}}$=-393000	$K_{\dot{v}}$=296000	$N_{\dot{v}} = 538000$
$X_{|u|u}$=-1960	$Y_{\dot{r}}$=-1.4$\times10^6$	$K_{\dot{r}}$=0	$N_{\dot{r}} = -4.395 + \times10^7$
X_{vr}=0.33m	$Y_{\dot{p}}$=-0.296$\times10^6$	$K_{\dot{p}}$=-0.674$\times10^6$	$N_{\dot{p}} = 0$
	$Y_{|u|v}$=-11800	$K_{|u|v}$=9260	$N_{|u|v} = -92000$
	Y_{ur}=-13100	K_{ur}=-102000	$N_{ur} = -4.71 \times 10^6$
	$Y_{|v|v}$=-3700	$K_{|v|v}$=29300	$N_{|v|v} = 0$
	$Y_{|r|r}$=0	$K_{|r|r}$=0	$N_{|r|r} = -202 \times 10^6$
	$Y_{|r|v}$=-0.794$\times10^6$	$K_{|r|v}$=0.621$\times10^6$	$N_{|r|v} = 0$
	$Y_{|v|r}$=-0.182$\times10^6$	$K_{|v|r}$=0.142$\times10^6$	$N_{|v|r} = -15.6 \times 10^6$
	$Y_{\phi|uv|}$=10800$\times10^6$	$K_{\phi|uv|}$=-8400	$N_{\phi|uv|} = -0.124 \times 10^6$
	$Y_{\phi u|r|}$=0.251$\times10^6$	$K_{\phi u|r|}$=-0.196$\times10^6$	$N_{\phi u|r|} = -4.98 \times 10^6$
	$Y_{\phi uu}$=-74	$K_{\phi|uu|}$=-1180	$N_{\phi u|u|} = -8000 \times 10^6$
		$K_{|u|p}$=-15500	$N_{|u|p} = 0$
		$K_{|p|p}$=-0.416$\times10^6$	$N_{|p|p} = 0$
		K_p=-0.5$\times10^6$	
		$K_{\phi\phi\phi}$=0	

REFERENCES

[1] T. Fossen, "A survey on nonlinear ship control: from theory to practice," Kidlington, UK, 2000, pp. 1 – 16.

[2] C. Kallstrom, K. Astrom, N. Thorell, J. Eriksson, and L. Sten, "Adaptive autopilots for tankers," *Automatica*, vol. 15, no. 3, pp. 241 – 54, 1979. [Online]. Available: http://dx.doi.org/10.1016/0005-1098(79)90042-6

[3] R. Reid and B. Mears, "Design of the steering controlled of a supertanker using linear quadratic control theory: a feasibility study," *IEEE Transactions on Automatic Control*, vol. AC-27, no. 4, pp. 940 – 2, 1982.

[4] C. G. Kallstrom, "Autopilot and track-keeping algorithms for high-speed craft," vol. 8, no. 2, 2000, pp. 185 – 190. [Online]. Available: http://dx.doi.org/10.1016/S0967-0661(99)00167-7

[5] V.-C. Nguyen, T.-O. Le, T.-B.-S. Do, M.-M. Nguyen, T.-M. Nguyen, T.-K.-T. Dinh, and T.-N. Man, "Study on an effective adaptive ship autopilot," in *Advanced Motion Control, 2004. AMC '04. The 8th IEEE International Workshop on*, march 2004, pp. 707 – 710.

[6] L. Moreira, T. I. Fossen, and C. Guedes Soares, "Path following control system for a tanker ship model," *Ocean Engineering*, vol. 34, no. 14-15, pp. 2074 – 2085, 2007.

[7] T. I. Fossen, "High performance ship autopilot with wave filter," in *Proceedings of the 10th International Ship Control Systems Symposium*, 1993, pp. 2271–2285.

[8] A. Bateman, J. Hull, and Z. Lin, "A backstepping-based low-and-high gain design for marine vehicles," *International Journal of Robust and Nonlinear Control*, vol. 19, no. 4, pp. 480 – 93, 2009. [Online]. Available: http://dx.doi.org/10.1002/rnc.1333

[9] A. Witkowska and R. Smierzchalski, "Nonlinear backstepping ship course controller," *International Journal of Automation and Computing*, vol. 6, no. 3, pp. 277 – 84, 2009. [Online]. Available: http://dx.doi.org/10.1007/s11633-009-0277-2

[10] E. McGookin, D. Murray-Smith, Y. Li, and T. Fossen, "Ship steering control system optimisation using genetic algorithms," *Control Engineering Practice*, vol. 8, no. 4, pp. 429 – 43, 2000. [Online]. Available: http://dx.doi.org/10.1016/S0967-0661(99)00159-8

[11] L. Morawski and J. Pomiriski, "Ship track-keeping experiments with a physical tanker model," *Control Engineering Practice*, 1998.

[12] S.-S. Hu, P.-H. Yang, J. Juang, and B. Chang, "Robust nonlinear ship course-keeping control by h i/o linearization and -synthesis," *International Journal of Robust and Nonlinear Control*, vol. 13, no. 1, pp. 55 – 70, 2003. [Online]. Available: http://dx.doi.org/10.1002/rnc.700

[13] B. Samanta and C. Nataraj, "Design of intelligent ship autopilots using particle swarm optimization," in *Swarm Intelligence Symposium, 2008. SIS 2008. IEEE*, sept. 2008, pp. 1 –7.

[14] S. Bhattacharyya, G. Rajesh, and D. K. Gupta, "Fuzzy autopilot for ship maneuvering," *International Shipbuilding Progress*, vol. 58, no. 4, pp. 191 – 218, 2011. [Online]. Available: http://dx.doi.org/10.3233/ISP-2012-0075

[15] N. H. Norrbin, "On the design and analysis of the zig-zag test on base of quasi linear frequency response," The Swedish State Shipbuilding Experimental Tank (SSPA), Tech. Rep. 104-3, 1963.

[16] M. I. Bech and L. W. Smith, "Analogue simulation of ship maneuvres," Hydro-Og and Aerodynamics Laboratory, Hy 14, 1969.

[17] M. Tomas-Rodriguez and S. Banks, "Linear approximations to nonlinear dynamical systems with applications to stability and spectral theory," *IMA Journal of Mathematical Control and Information*, vol. 20, no. 1, pp. 89 – 103, 2003. [Online]. Available: http://dx.doi.org/10.1093/imamci/20.1.89

[18] M. Tomas-Rodriguez and S. P. Banks, *Linear, Time-varying Approximations to Nonlinear Dynamical Systems: with Applications in Control and Optimization*, Springer, Ed., 2010, vol. 400, no. XII.

[19] M. Tomas-Rodriguez, C. Navarro-Hernande, and S. Banks, "Parametric approach to optimal nonlinear control problem using orthogonal expansions," vol. 16, Prague, Czech republic, 2005, pp. 556 – 561.

[20] C. Hernandez, S. Banks, and M. Aldeen, "Observer design for nonlinear systems using linear approximations," *IMA Journal of Mathematical Control and Information*, vol. 20, no. 3, pp. 359 – 70, 2003.

[21] T. Cimen and S. Banks, "Nonlinear optimal tracking control with application to super-tankers for autopilot design," *Automatica*, vol. 40, no. 11, pp. 1845 – 63, 2004. [Online]. Available: http://dx.doi.org/10.1016/j.automatica.2004.05.015

[22] T. Pérez, *Ship Motion control Course keeping and roll Stabilisation using rudder and fins*. Springer, 2005.

[23] SNAME, "Nomenclature for treating the motion of submerged body through a fluid," The Society of Naval Architects and Marine Engineers, Technical and Research bulletin 1-5, 1950.

[24] T. Perez, A. Ross, and T. I. Fossen, "A 4-dof simulink model of a coastal patrol vessel for manoeuvering in waves," in *Manoeuvring and Control of Marine Craft (MCMC 2006)*, Lisbon, 2006.

[25] M. Blanke, "Ship propulsion losses related to automated steeering and prime mover control," Ph.D. dissertation, The University of Denmark Lyngby., 1981.

[26] N. Norrbin, "Theory and observation on the use of a mathematical model for ship manoeuvring in deep and confined waters," *8th Symposium on Naval Hydrodynamics, USA*, 1970.

[27] E. V. Lewis, *Principles of Naval Arquitecture*. The Society of Naval Architects and Marine Engineers, 1989.

[28] V. Bertram, *Practical ship hydrodynamics*, 2nd ed. Oxford: Butterworth-Heinemann, 2012, volker Bertram.

[29] J. Van Amerongen, "Adaptive steering of ships-a model reference approach," *Automatica*, vol. 20, no. 1, pp. 3 – 14, 1984.

[30] T. I. Fossen, *Guidance and Control of Ocean Marine Vehicles*. John Wiley and Sons Ltd, 1994.

[31] T. Fossen, *Marine Control Systems: Guidance, Navigation and Control of Ships, Rigs and Underwater Vehicles*. Marine Cybernetics, 2002.

[32] T. I. Fossen and T. Perez. (2004) Marine systems simulator (mss).

[33] J. van Amerongen, "Adaptive steering of ships: a model- reference approach to improved manoeuvring and economical course keeping," Ph.D. dissertation, 1982.

[34] K. J. Astrom and T. Hagglund, *Advanced PID control*. Research Triangle Park, NC: ISA- The Instrumentation, Systems, and Automation Society, 2006, karl J. Astrom, Tore Hagglund.

[35] K. Ogata, *Modern control engineering*, 5th ed. Boston, MA: Prentice-Hall, 2010.

[36] R. Brayton and G. Hachtel, "A new algorithm for statistical circuit design based on quasi-newton methods and function splitting," *IEEE Transactions on Circuits and Systems*, vol. CAS-26, no. 9, pp. 784 – 94, 1979.

[37] E. Revestido, E. Moyano, F. J. Velasco, and E. Lpez, "Tuning heading controllers of an autonomous in-scale fast-ferry model," in *Maritime Transport IV*, 2009.